Available online at www.sciencedirect.com
ScienceDirect
Journal of Organometallic Chemistry 692 (2007) 1198–1215
Journal of Organometallic Chemistry
www.elsevier.com/locate/jorganchem

Review

Crystallography of vitamin B_{12} proteins

Lucio Randaccio *, Silvano Geremia, Jochen Wuerges

Centre of Excellence in Biocrystallography, Department of Chemical Sciences, University of Trieste, Via L. Giorgieri 1, 34127 Trieste, Italy

Received 16 September 2006; received in revised form 27 November 2006; accepted 27 November 2006
Available online 3 December 2006

Abstract

This review deals with results from crystallographic studies on proteins that interact with the essential micronutrient cobalamin (vitamin B12). Both B12-dependent enzymes and B12-transport proteins are described with an emphasis on structural aspects of cobalamin and its protein environment.
Published by Elsevier B.V.

Keywords: X-ray crystallography; Cobalamin; Vitamin B12-dependent enzymes; Vitamin B12 transport; Cobalt–carbon bond

Contents

1. Introduction . . . 1198
2. Methyltransferases . . . 1201
   2.1. Structure and function of methionine synthase (MetH) . . . 1201
   2.2. Methanol–cobalamin methyltransferase . . . 1204
3. Structural aspects of AdoCbl enzymes . . . 1205
   3.1. Class I and III enzymes (isomerases) . . . 1206
   3.2. Class II enzymes . . . 1208
   3.3. B_{12} ribonucleotide reductase . . . 1210
4. Adenosyltransferase . . . 1211
5. Vitamin B_{12} transport proteins . . . 1211
6. Conclusions . . . 1213
   References . . . 1214

1. Introduction

Pernicious anaemia (PA), first observed in 1824, was a fatal disease until the 1920s, when it was discovered that raw liver contained a substance, the antiPA factor, which reverses this anaemia in dogs and humans [1]. In mammals, deficiency of this factor also provokes severe neurological diseases, particularly in the elderly population. The 'liver factor', later named vitamin B_{12}, was extracted and crystallized in 1948 [2,3]. Since then, crystallography has played a fundamental role in the development of knowledge of the chemistry and biochemistry of vitamin B_{12} (Table 1). This role started with the landmark crystal structure of vitamin B_{12} or cyanocobalamin (CNCbl) [4,5], which allowed the upsurge of vitamin B_{12} chemistry, up to

* Corresponding author.
E-mail address: randaccio@univ.trieste.it (L. Randaccio).

0022-328X/$ - see front matter Published by Elsevier B.V.
doi:10.1016/j.jorganchem.2006.11.040

Table 1
Historical outline of the impact of crystallography in vitamin B_{12} research

Early medicinal age	
1824	First observation of pernicious anaemia
1926	Treatment of pernicious anaemia with liver (*Minot and Murphy*)
1934	*Nobel prize in medicine to Whipple, Minot and Murphy*
Vitamin B_{12} crystallographical age	
1948	Isolation and crystallization of vitamin B_{12}
1956-7	X-ray structure of vitamin B_{12}, cyanocobalamin (*CNCbl*)
1961	X-ray structure of the B_{12} coenzyme, *adenosylcobalamin* (*AdoCbl*)
1964	*Nobel Prize in chemistry to Dorothy Hodgkin*
1972	Total synthesis of vitamin B_{12}
1985	X-ray structure of *methylcobalamin* (*MeCbl*)
Protein crystallographical age	
1994	X-ray structure of MeCbl-binding domains of *methionine synthase* (*MetH*)
1996	X-ray structure of *methylmalonyl-coenzyme A mutase* (*MMCM*)
1999	X-ray structure of *diol dehydratase* (*DD*)
1999	X-ray structure of *glutamate mutase* (*GLM*)
2001	X-ray structure of *ATP:co(I)rrinoid Adenosyltransferase* (*CobA*)
2002	X-ray structure of *glycerol dehydratase* (*GD*)
2002	X-ray structure of *ribonucleotide triphosphate reductase* (*RTPR*)
2003	X-ray structure of *BtuB*
2004	X-ray structure of substrate-binding domains of *methionine synthase*
2004	X-ray structure of *lysine 5,6-aminomutase* (*5,6-LAM*)
2006	X-ray structure of *transcobalamin* (*TC*)
New medicinal age	
	B_{12} conjugates as potential anti-tumoural and imaging drugs

the recent crystal structure of several B_{12}-dependent enzymes, which has provoked an enormous increase in work on vitamin B_{12} enzymology [6,7]. Finally, the recent X-ray structure of transcobalamin (TC) [8] has furnished the structural basis for designing appropriate Cbl-based bioconjugates for imaging of tumours as well as targeted and selected delivery of anti-tumour agents to malignant cells [9,10]. CNCbl belongs to a group of strictly related compounds called cobalamins (Fig. 1). Cobalamins are octahedral Co(III) complexes, equatorially coordinated by a corrin ligand which bears seven amide side chains a–g. Chain f is connected through an amide bond to a nucleotide, whose dimethylbenzimidazole may coordinate Co at one axial position on the α side or lower side (base-on form) or, upon protonation, may be displaced by an exogenous ligand (base-off form). The various cobalamins differ in the axial ligand X on the β side or upper side (Fig. 1).

CNCbl is not biologically active in mammals, whereas MeCbl is involved in methionine biosynthesis and AdoCbl (Fig. 1) in the reversible isomerisation of L-methylmalonyl into a succinyl residue catalyzed by the L-methylmalonyl-CoA mutase (MMCM) [11,12]. They are the only cofactors so far known containing a metal–carbon bond involved in the enzymatic processes. Mammals are not able to synthesize cobalamins, which thus must be supplied with the diet. Consequently, they have developed a complex pathway for absorption, blood transportation and cellular uptake of dietary Cbl (Fig. 2, left side). The delivery from food to tissues involves three successive transport proteins, which form a tight complex with Cbl, and cell surface receptors for these protein–Cbl complexes [13,14]. After release of Cbl from its complex with TC in lysosomes, cobalamin is transformed to the MeCbl and AdoCbl coenzymes (Fig. 2, right side) in the cytosol and in the mitochondrion, respectively [15].

MeCbl-based methyltransferases catalyze the transfer of methyl groups. The most studied is methionine synthase (MetH), which catalyzes the methyl transfer from *N*-methyltetrahydrofolate ($MeH_4Folate$) to Cob(I)alamin for onward transmission from the formed MeCbl to homocysteine to produce methionine. The enzymatic mechanistic scheme requires a series of nucleophilic displacements of a methyl group, which can be considered as a formal heterolytic Co–Me bond formation and cleavage [16]. MeCbl is also a cofactor in the carbon dioxide fixing pathway in anaerobic acetogenic bacteria [17] and methanogenic archaea [18]. Cobalamins are also found to be coenzymes in the reductive dehalogenases, enzymes of anaerobic bacteria, which are able to reductively dechlorinate aliphatic and aromatic chloro-hydrocarbons [7,12].

AdoCbl (coenzyme B_{12}) is the cofactor in several enzymes, including MMCM, which catalyzes the intramolecular 1,2 shift of a H atom and an electronegative group. The rearrangement is a stepwise process initiated by the homolytic cleavage of the Co–C bond, to give the Cob(II)alamin and adenosyl radicals, and terminates with the reformation of this bond.

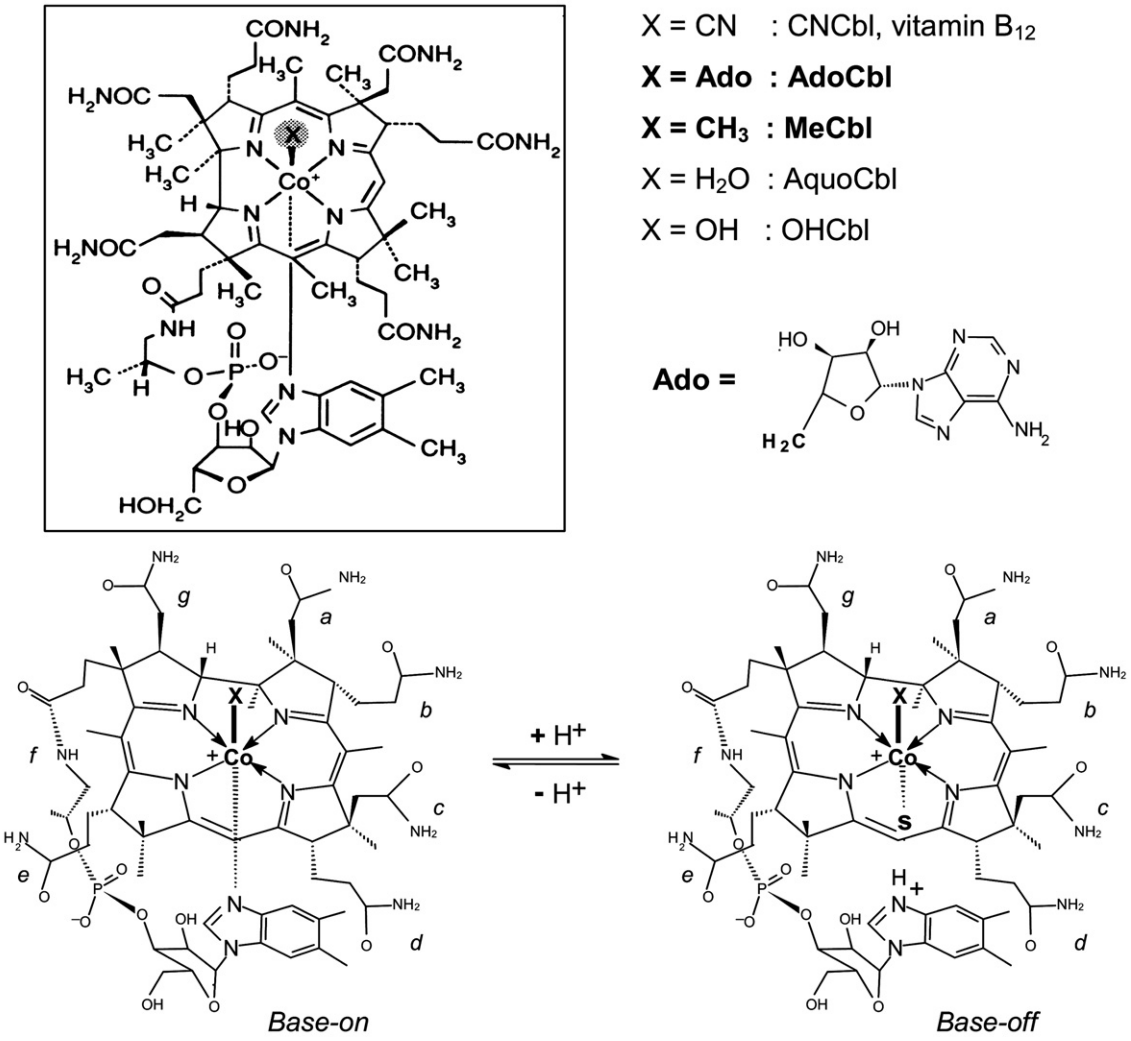

Fig. 1. Vitamin B_{12} or cyanocobalamin (CNCbl) and biologically active cobalamins (in bold characters). *S* denotes a substituent, e.g. an imidazole nitrogen from a histidine residue of a protein.

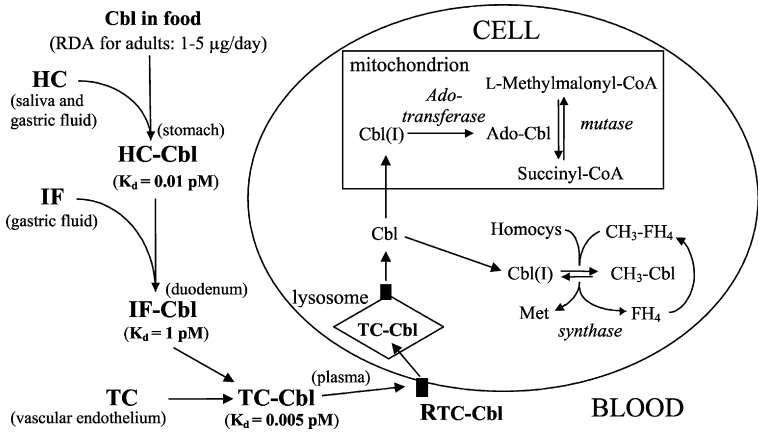

Fig. 2. Absorption, cellular uptake and enzymatic processes involving cobalamins (Cbl) in mammals. The intracellular trafficking to the two mammalian Cbl-dependent enzymes has been reviewed recently [15].

A complete survey on the chemistry and enzymology of vitamin B_{12} has recently been given by Kenneth Brown in his exhaustive review [7] covering all the work done from 1999 up to 2004. The crystallography of cobalamins has also been recently reviewed up to 2005 [19]. This review focuses on the crystallography of B_{12} proteins, including

the first X-ray structure of a mammalian B_{12}-transporting protein, transcobalamin, in complex with cobalamin (TC–Cbl) [8]. The accurate geometry of the axial fragment of the isolated CN-, Me- and AdoCbl is given in Table 2, together with other properties of the Co–C bond.

2. Methyltransferases

2.1. Structure and function of methionine synthase (MetH)

An important role for cobalamin lies in some methyl transfer reactions, among which the best studied is the methyltransferase MetH [16], present in mammals and in many bacteria. This enzyme catalyzes the transfer of a methyl group from N^5-methyl-tetrahydrofolate (CH_3–H_4Folate) to homocysteine to form methionine. Cbl, as cob(I)alamin, accepts the methyl from CH_3–H_4Folate (Fig. 3, reaction 1) and then transfers it, as MeCbl, to homocysteine (reaction 2), so that the cofactor cycles between MeCbl and Cob(I)alamin during the catalytic turnover. Occasionally Cob(I)alamin becomes oxidized and thereby converted to inactive Cob(II)alamin. The latter species is then returned to the catalytic cycle by reductive methylation to MeCbl with a flavodoxin-reducing agent and *S*-adenosylmethionine alkylating agent, AdoMet (reaction 3). All these reactions are performed, as sketched in Fig. 3, by the modular MetH enzymes from *Homo sapiens* and *Escherichia coli* (with a molar mass of about 136 kDa), which consists of the four functional modules shown in Fig. 4.

The structure of full-length MetH is not available, but a "divide-and-conquer" strategy involving expression and/or isolation of the modular fragments furnished structural insight and allowed to delineate not only the structural organization, but also several functional aspects of MetH, which could not have been obtained from the knowledge of the three-dimensional structure of complete MetH alone. The two N-terminal domains constitute the homocysteine (Hcy)-binding domain and CH_3–H_4Folate-binding domain (Fol), respectively. The N-terminal fragment of MetH, comprising these two domains, has been expressed and both the form with and without substrate were crystallographically characterized [20]. Both domains show the typical $(\beta/\alpha)_8$ TIM barrel that is generally found for substrate-binding domains of B_{12} enzymes (Fig. 5) and that resembles the analogous domain found in triosephosphate-isomerase (TIM). The two domains are firmly associated

Table 2
Some physico-chemical properties and distances in the axial fragment of CN-, Me- and AdoCbl ($E_{1/2}$ for Co(III) → Co(II), BDE = Co–C bond dissociation energy in kJ/mol)

R	Co–C (Å)	Co–NB3 (Å)	Co–C–C (°)	$\nu_{Co\text{-}C}$ (cm^{-1})[a]	$E_{1/2}$ (V)[b]	BDE[c]
CNCbl[d]	1.886(4)	2.041(3)	180.0(1)	–	–	–
MeCbl	1.979(4)[d]	2.162(4)[d]	–	506	−1.60	155 ± 12
AdoCbl	2.030(3)[e]	2.237(3)[e]	123.4(2)	430	−1.35	125 ± 8

[a] Ref. [78].
[b] Ref. [79].
[c] Ref. [80].
[d] Ref. [81].
[e] Ref. [82].

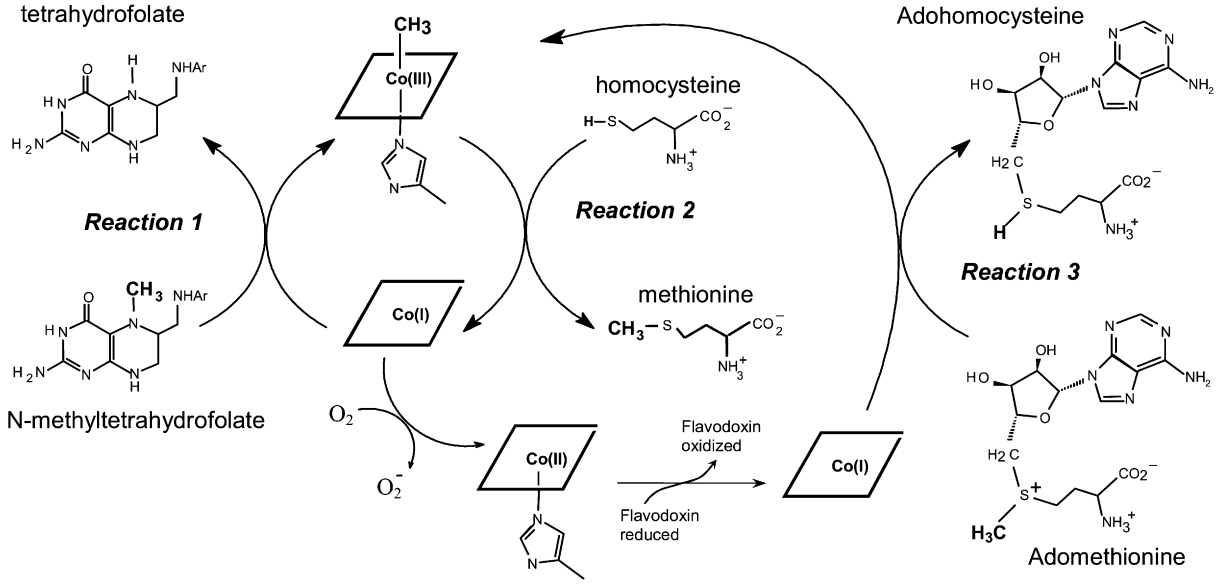

Fig. 3. The catalytic cycle and coenzyme re-activation reaction in methionine synthase.

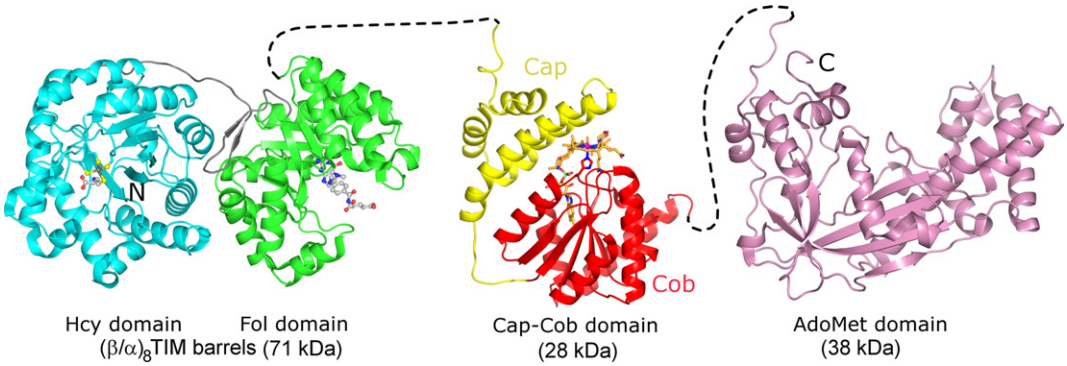

Fig. 4. Overview of the modular architecture of methionine synthase. The two N-terminal modules are $(\beta/\alpha)_8$ TIM barrels (PDB accession code 1Q8 J); the Cap-Cob module (PDB code 1BMT) shows a α/β Rossmann fold in the Cob (B_{12}-binding) domain. The C-terminal module (PDB code 1K7Y) is the AdoMet domain involved in the re-activation reaction 3 (see Fig. 3).

and resist proteolysis even in the presence of 3% trypsin. The barrel axes are oriented perpendicularly to each other. The domain interface is relatively hydrophobic and incorporates a large part of the connecting linker, forming about 20 H-bonds in addition to van der Waals interactions. The Hcy binding domain contains a zinc ion as essential cofactor. When homocysteine enters the active site, it coordinates, likely as thiolate [21], the zinc ion. Three Cys residues complete the distorted tetrahedral geometry around the zinc ion (Fig. 5B).

The third module, comprising the Cap and Cob domains, can be obtained by digestion of the protein with trypsin and represents the binding site of cobalamin. The X-ray crystal structure of this fragment, the first ever determined for a Cbl-dependent protein, led to the discovery of the base-off/His-on binding mode (see below) [22] (Fig. 6A). It consists of two domains and comprises a four-helix

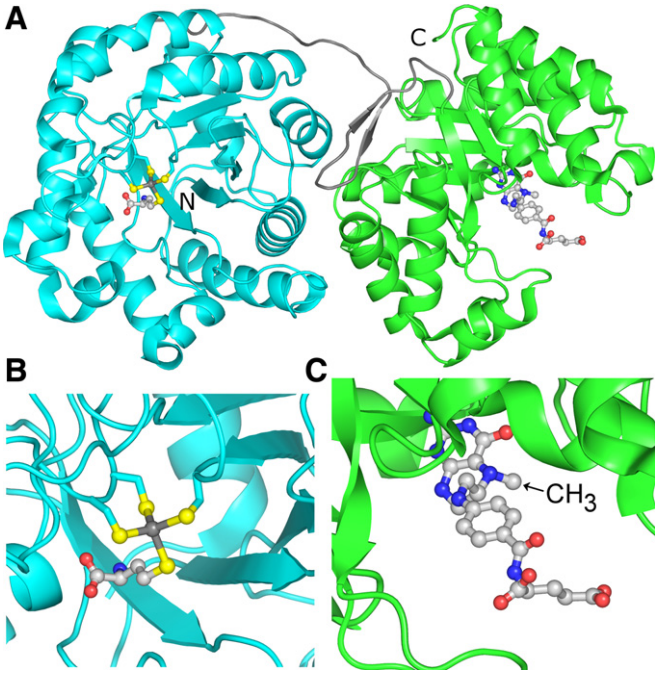

Fig. 5. (A) Hcy domain (in cyan) and Fol domain (in green) of methionine synthase (MetH, PDB code 1Q8 J). (B) Enlarged view to the homocysteine ligand which, together with three cysteine residues of the enzyme, coordinates a metal ion (in grey). Sulphur atoms are shown as yellow spheres. (C) Enlarged view to the methyl–H_4Folate in the Fol domain, evidencing the methyl group to be transferred.

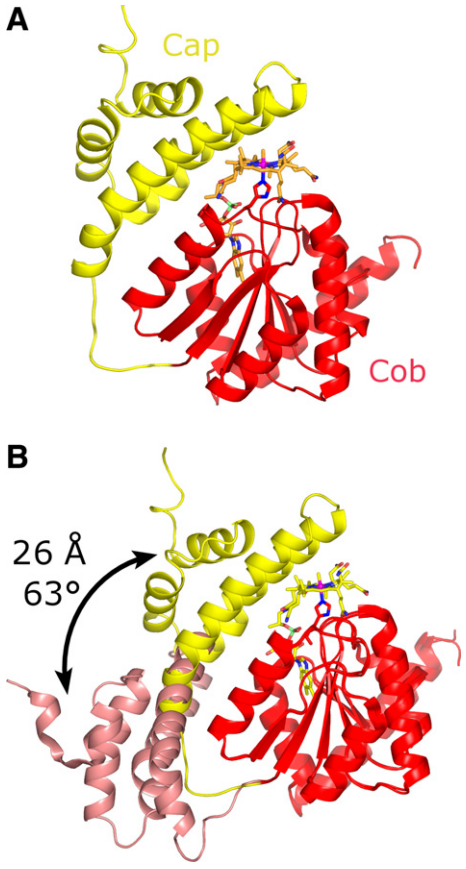

Fig. 6. Different conformations of the Cap-Cob module in methionine synthase. (A) The Cap domain (in yellow) and the Cob domain (in red) (PDB code 1BMT) and (B) superposition of the Cob domains reveals the movement of the Cap domain relative to the Cob domain as indicated by the arrow. The Cap domain in yellow corresponds to the structure of the isolated Cap-Cob module and the one in pink corresponds to the structure of the Cap-Cob module in the re-activation conformation (PDB code 1K7Y). In the latter conformation, His 759 is assumed to dissociate from the Co since a loop from the AdoMet domain wedges cobalamin away from the Cob domain towards the AdoMet domain [24].

bundle (Cap) and an α/β Rossmann motif (Cob), which sandwiches the cobalamin in the base-off form. Cobalamin is covered on its β side by the Cap domain and its nucleotide chain is embedded in the Cob domain. The dimethylbenzimidazole moiety is displaced by an imidazole of the histidine residue 759, which coordinates to cobalt on the α side. The fourth module, AdoMet, contains the *S*-adenosyl-L-methionine (AdoMet) binding site and represents the activation domain of MetH. An X-ray structure has shown that the activation domain adopts an unusual helmet-shaped conformation, with AdoMet located on its inner surface [23]. Expression and X-ray structure determination of the two C-terminal modules [24], Cap-Cob and AdoMet, demonstrated that large conformational changes occur in the former module, when it binds the latter. The Cap domain moves 26 Å and rotates by 63°, with respect to its position in the isolated Cob-Cap module, thereby uncovering the β face of cobalamin and enabling Co to approach the AdoMet substrate in the activation domain (Fig. 6B). A fragment of MetH, deprived of the AdoMet module, initially catalyzes the overall reaction as the full-length enzyme, but slowly loses activity and cannot be reactivated by exogenous AdoMet and the reductant.

According to the scheme in Fig. 3, the Cap-Cob module must approach the Fol domain when the methyl is transferred from CH_3–H_4Folate to Cob(I)alamin (reaction 1) and the Hcy domain when the methyl is transferred from MeCbl to homocysteine (reaction 2). Accidentally produced inactive Cob(II)alamin can be recovered as active MeCbl in the activation cycle by reductive methylation (reaction 3). Thus, the enzyme function involves the chemistry of cobalamin in three different oxidation and coordination states.

Due to its modular nature, the enzyme must undergo conformational changes in order to allow the binding domains of the different substrates to access the cobalamin-binding domain in the three methyl transfer reactions (Fig. 3). The effect of substrate or product concentration on

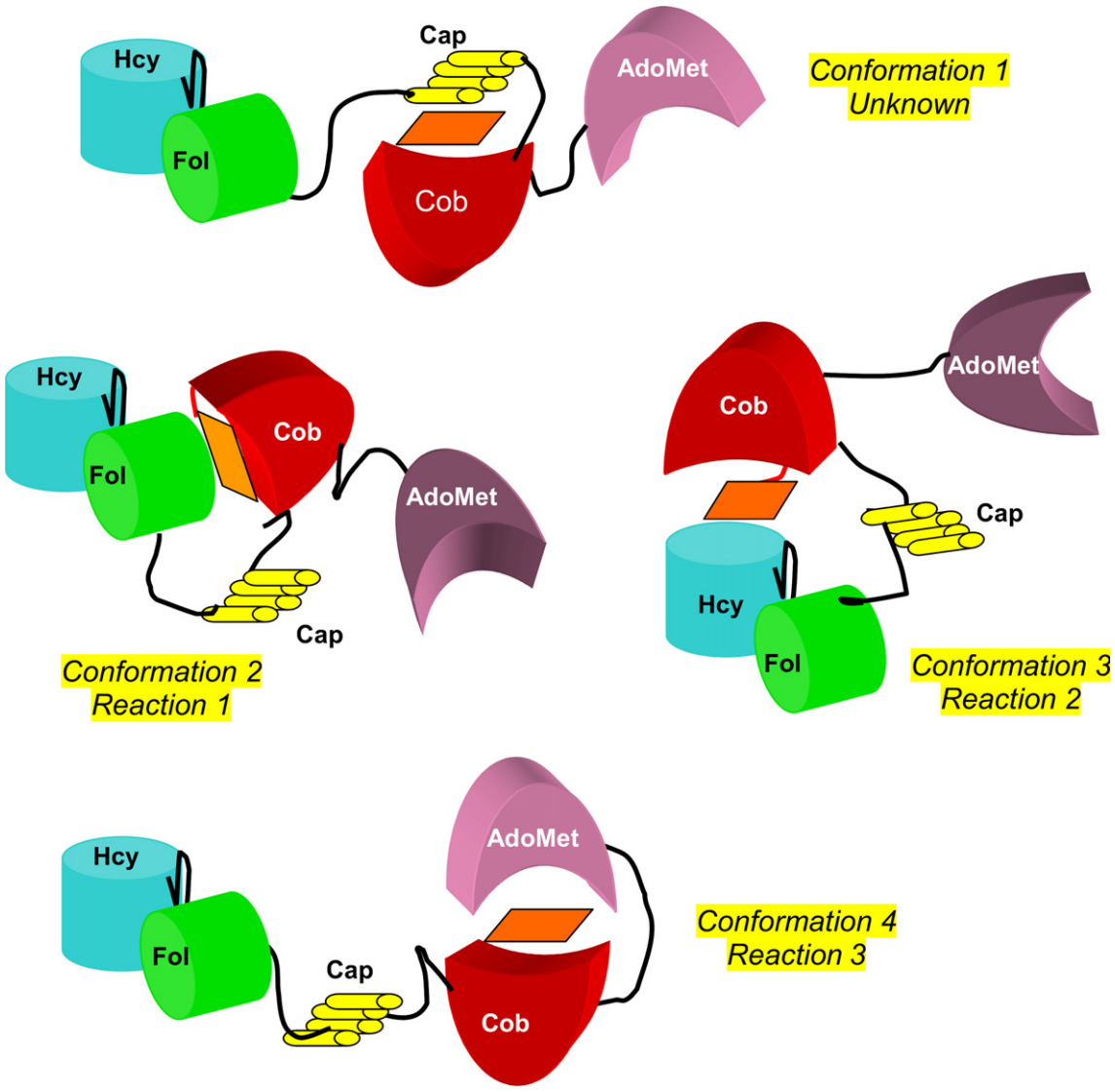

Fig. 7. Scheme of four possible conformations in methionine synthase (MetH) and their corresponding function [25].

the distribution of MetH conformations was analyzed in an impressive work on the full length MetH, its expressed fragments and their mutants [25]. The differences in the UV/visible spectra of methylcobalamin in the different states (base-on/base-off) were exploited to relate the ligand environment of enzyme-bound cobalamin to the enzyme conformation. Thanks also to the available structural information, the results of this work suggest that MetH can be described in solution as an ensemble of at least four conformational states (Fig. 7) and that the distribution of the conformers is strongly influenced by differential binding of the substrates/products, according to the particular reaction to be catalyzed. Thus, at any instant only one of the substrate-binding domains may interact with the Cap-Cob domain. For example, during the catalytic cycle the Cap-Cob domain must travel back and forth between the Fol and Hcy domains, separated by about 50 Å, and MetH passes from the conformational state 2 to the conformational state 3 and *vice versa*, since it is likely that the Fol and Hcy domains do not easily dissociate (see above and Fig. 7) [20].

The importance of the Zn ion in the methyl transfer from MeCbl to homocysteine has been addressed by a DFT study [26] which modelled the reaction using a simple model, $CH_3Co(corrin)Im^+$ as MeCbl, and CH_3S^- as the substrate. The corrin ligand is shown in Fig. 8A and derives from Cbl by substituting all side chains by H atoms. Calculations suggested that the reaction (Fig. 8B) is strongly exothermic in vacuum, but much less in water. More importantly, the free activation energy was calculated at 25 °C to be 104 kJ/mol in aqueous solution, which is in excellent agreement with the experimental value of 100 kJ/mol in water, whereas in the enzyme the barrier is 61 kJ/mol. If the protonated substrate CH_3SH is used, the value of the barrier is calculated to be 197 kJ/mol. Thus, deprotonation of homocysteine appears to be necessary to favour the reaction, in agreement with kinetic experiments in solution [27]. However, the calculations may underestimate the height of the barrier in the enzyme since a free thiolate is probably less nucleophilic when coordinated to a zinc ion.

2.2. Methanol–cobalamin methyltransferase

In the energy metabolism of methanogenic archaea, methanol can be reduced to methane or oxidized to CO_2 with methyl–CoM as intermediate. The methanol:CoM methyltransferase MtaABC catalyzes the formation of this intermediate and is built of three subunits. MtaC binds the cofactor cob(I)amide and presents it to MtaB for transfer of the methanol-derived methyl. MtaA then transfers the methyl from MtaC-bound methyl-cob(III)amide to CoM.

The structure of the substrate-free complex MtaBC from *Methanosarcina barkeri* shows the zinc-containing MtaB with a TIM barrel fold and MtaC with bound 5-hydroxybenzimidazolylcobamide at 2.5 Å resolution ([28], PDB code 2I2X). MtaC is similar to the Cap-Cob module of MetH with which it shares 35% sequence identity. The orientation of the small α-helical domain with respect to the Rossmann domain resembles that in the re-activation conformation of MetH rather than the "as-isolated" conformation (Fig. 6B). In MtaC, contacts of cobamide are present to its MtaB partner and to a symmetry-related MtaB in the tetrameric $(MtaBC)_2$ organisation. The structure reveals a Co ion coordinated by His 136 which displaced the 5-hydroxybenzimidazole base as ligand on the lower axial side. An upper axial ligand is not observed, i.e. the Co ion is pentacoordinate. This points to the Co(II) oxidation state as a result of X-ray-induced reduction during data collection of the initial cob(III)amide in MtaC (prepared under aerobic conditions).

The Zn(II) is found almost in line with the Co centre and the coordinating Nε of His 136 and is located at a distance to Co (7.7 Å) which leaves space for the substrate methanol to be tentatively modelled into the structure. In this scenario, the hydroxyl of methanol may fill the empty fourth coordination site of the electrophile Zn(II) and may be activated for the subsequent nucleophilic attack on the methyl

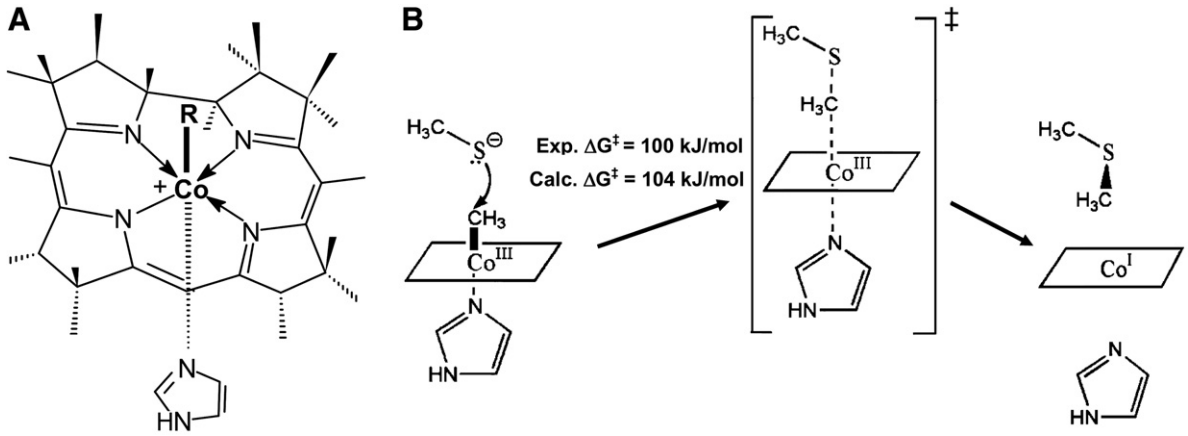

Fig. 8. (A) The simple corrin model R-$Co(corrin)Im^+$ used for DFT studies. R is Ado or CH_3. (B) The energy barrier in the methyl transfer from MeCbl to homocysteine in aqueous solutions at 25 °C.

group by the base-off Co(I) to generate methyl-Cob(III)amide in base-on form.

3. Structural aspects of AdoCbl enzymes

Although the catalyzed reactions are quite different, all the AdoCbl-dependent enzymes, except for ribonucleotide reductase, share a common feature. They catalyze the intramolecular 1,2 shift of a H atom with a generally electronegative group, accomplishing isomerisation reactions that are difficult to achieve by typical reactions in organic chemistry [29,30]. According to Toraya [31] they are grouped in three classes as shown in Table 3, on the basis of the specifics of the migrating group and the receiving carbon as well as of other cofactors in addition to Cbl, such as potassium ions in Class II and pyridoxal-5′-phosphate in Class III. Class I enzymes are mutases, which act reversibly; Class II enzymes include lyases (such as dehydratases and deaminases) and the ribonucleotide reductase. These enzymes are sometimes denominated eliminases since they catalyze the 1,2 shift of the H atom with an OH or NH_2 group with subsequent elimination of water or ammonia and the irreversible formation of the corresponding aldehyde. Class III enzymes are aminomutases.

From a structural point of view these three classes can be grouped into two categories, depending on the AdoCbl coenzyme form. The Class I mutases and Class III aminomutases bind AdoCbl in base-off form, with the α axial position occupied by the imidazole of a histidine residue, known as ''base-off/His-on'' binding. They all contain the consensus sequence, Asp-x-His-x-x-Gly, which includes the axial His residue, as it was first discovered for MeCbl in the Cbl-binding domain of methionine synthase, shown in Fig. 6 [22]. All Class II enzymes bind AdoCbl in base-on form with the benzimidazole group coordinated to Co in the α axial position. Several X-ray structures of Class I and Class II enzymes have been reported, and recently one of a Class III aminomutase.

The generally accepted enzymatic mechanism for methylmalonyl-CoA mutase is sketched in Fig. 9. After binding of the substrate, the reaction starts with the Co–C bond homolysis and formation of the Ado- and Cob(II)alamin

Table 3
Reactions catalyzed by the AdoCbl enzymes (with EC numbers given in parenthesis)

Class I enzymes			
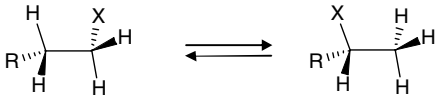			
Glutamate mutase (5.4.99.1)	$X = CH(NH_3^+)COO^-$	$R = CO_2^-$	
Methylmalonyl-CoA mutase (5.4.99.2)	$X = COSCoA$	$R = CO_2^-$	
2-Methyleneglutamate mutase (5.4.99.4)	$X = C(=CH_2)COO^-$	$R = CO_2^-$	
Isobutyryl-CoA mutase (5.4.99.13)	$X = COSCoA$	$R = H$	\
Class II enzymes			
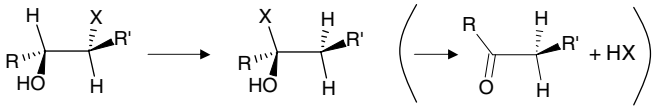			
Diol dehydratase (4.2.1.28)	$X = OH$	$R = H$	$R' = CH_3$, H, CH_2OH
Glycerol dehydratase (4.2.1.30)	$X = OH$	$R = H$	$R' = CH_2OH$, CH_3, H
Ethanolamine ammonia-lyase (4.3.1.7)	$X = NH_3^+$	$R = H$	$R' = H$, CH_3
Ribonucleotide reductase (1.17.4.2)	$X = OH$(left), H(right)	$R =$ C-4′ of ribonucleotide	$R' =$ C-1′ of ribonucleotide
Class III enzymes			
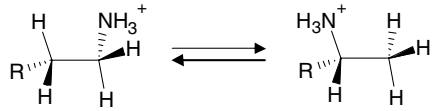			
L-β-lysine [D-lysine] 5,6-aminomutase (5.4.3.3)		$R = CH_2CH(NH_3^+)CH_2COO^-$, $(CH_2)_2CH(NH_3^+)CH_2COO^-$	
D-Ornithine 4,5-aminomutase (5.4.3.5)		$R = CH_2CH(NH_3^+)COO^-$	

All reactions occur in bacteria, and the methylmalonyl-CoA-mutase reaction occurs also in mammals.

radicals. The Ado-radical abstracts a H atom from the substrate to produce a substrate radical and 5′-deoxyadenosine. The substrate radical next rearranges into a product radical which then abstracts a H atom from 5′-deoxyadenosine to form the product, which is released, and the so formed Ado· radical restores the Co–Ado bond. The means by which these enzymes catalyze the simple dissociation of the Co–C bond of AdoCbl about 10^{12} times faster than the free coenzyme is unknown and remains the topic of intense research, as it has been in the past already [7,19].

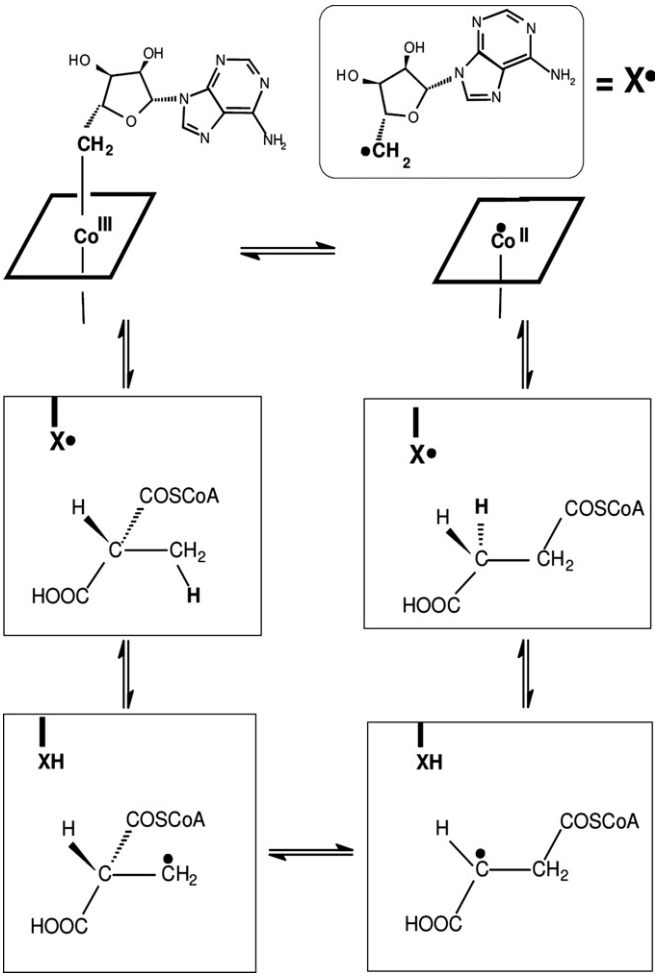

Fig. 9. The catalytic cycle in MMCM.

3.1. Class I and III enzymes (isomerases)

The first X-ray structure of an Ado-based enzyme was that of methylmalonyl-CoA mutase (MMCM) from *P. shermanii* in complex with AdoCbl and the partial substrate desulpho-CoA at 2.0 Å resolution [32]. Desulpho-CoA lacks the succinyl group and with respect to the 'true' substrate, the terminal thiol group is substituted by a H atom. This enzyme, which catalyzes the interconversion sketched in Fig. 9, is an αβ heterodimer of 149 kDa, where the α and β chains have similar fold. However, desulpho-CoA and AdoCbl bind only the α chain (Fig. 10). In contrast, the human MMCM is an α_2 homodimer of 150 kDa, each subunit having one substrate-binding site and one Cob domain [33]. The cobalamin-binding site is very similar to the Cob domain found in MetH (Fig. 6), where the cobalamin binds to the protein in the base-off/His-on mode. The substrate binding domain, as usually found in B_{12} enzymes, is a $(\beta/\alpha)_8$ TIM barrel, similar to those shown in Fig. 5. However, no electron density for the adenosyl group was detected, suggesting that the coenzyme is present in the reduced Cob(II)alamin form, after having lost the adenosyl radical during crystallization or X-ray data collection. On the contrary, the substrate-free holoenzyme structure at 2.7 Å resolution clearly showed the intact AdoCbl, where the adenine moiety stacks with the side chain of the Tyr A89 residue close to the substrate binding site [34]. The comparison of the latter structure to that with desulpho-CoA substrate also indicates that large conformational changes occur when the substrate binds the protein. Particularly, the TIM barrel domain is split apart and the active site is accessible to solvent in the substrate-free structure. When the substrate binds, the barrel encloses the substrate and the active site is completely buried. Finally, the structure of MMCM with a methylmalonyl-CoA/succinylCoA mixture (50%) in the active site was reported together with those with two inhibitors (all at

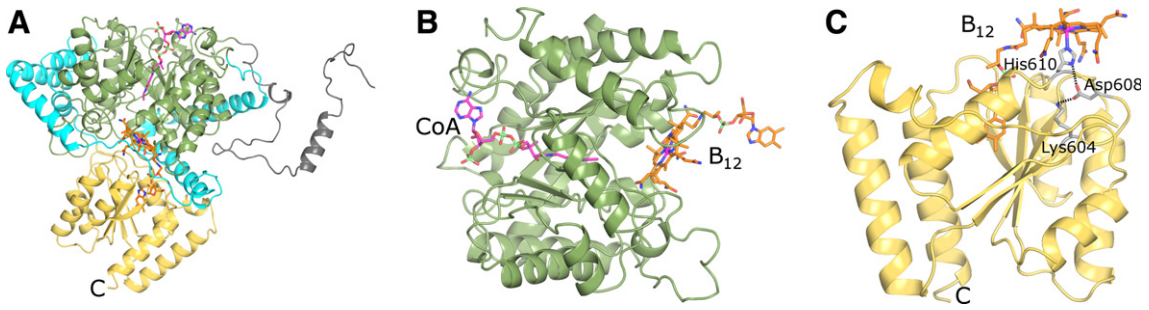

Fig. 10. The MMCM structure (PDB code 1REQ). (A) Shown here is the α-subunit in the heterodimeric enzyme. It contains a $(\beta/\alpha)_8$ TIM barrel coloured in green and a C-terminal domain (in yellow) with the topology of the Cob domain of MetH. (B) Enlarged view to the TIM barrel with the desulpho-coenzyme A (CoA, in magenta) and the base-off cobalamin (in orange). (C) The C-terminal domain provides the His residue which coordinates to the Co from the lower axial side. This histidine is stabilized by a H-bond network involving an aspartate and a lysine.

2.2 Å resolution) [35], which showed electron density for partial occupancy of a 5′-deoxyadenosine not coordinated to cobalt and with its 5′-carbon atom near the substrate. This structural result supports the previous suggestion [36,37] that the entrance of the substrate significantly contributes to the enhancement of the Co–C bond homolysis of more than 12 orders of magnitude in the enzyme with respect to the free coenzyme. In fact, the binding of the substrate induces severe conformational changes in the protein [32,34], with the closing up of the TIM barrel about the substrate, which provokes a further activation of the Co–C bond, in addition to that resulting from the binding of AdoCbl to the protein scaffold.

Glutamate mutase (GLM) catalyzes the reversible conversion of *S*-glutamate to 2*S*,3*S*-methylaspartate (Table 3) according to the following reaction:

$$^{-}O_2C(NH_3^+)–CH–CH_2CO_2^- \rightleftarrows {}^{-}O_2C(NH_3^+)–CH–CH(CH_3)CO_2^-$$

The X-ray structures of a recombinant GLM (136 kDa) from *Clostridium cochlearium* reconstituted with CNCbl and MeCbl at 88 K (1.6 and 2.0 Å resolution, respectively) have been reported [38]. The enzyme is a heterotetramer $\varepsilon_2\sigma_2$, in which each heterodimer contains a full cobalamin molecule and a tartrate ion from the crystallization buffer located in the presumed active site (Fig. 11). The σ chain (MutS) has the usual α/β fold of the base-off/His-on Cbl-binding domain, with the nucleotide moiety embedded in the five β strands, which are surrounded by six α helices as found in MetH and MMCM (Fig. 6). The ε subunit is a $(\beta/\alpha)_8$ TIM barrel packing against the β face of cobalamin, which approaches the tartrate ion inside the TIM barrel cavity (Fig. 11B).

The NMR solution structures [39,40] of the AdoCbl-binding subunits MutS in the apo- and holoform were shown to have secondary and tertiary structures quite similar to each other and to those of the X-ray structure.

The question of the Co axial distances was also addressed thanks to the relatively high resolution of the two CNCbl- and MeCbl-reconstituted GLM structures [38]. In fact, an anomalously long Co–N axial bond of 2.5 Å as compared to those found in free alkylcobalamins (⩽2.2 Å [19]) was found in previous structures of B_{12} enzymes. The geometry of the axial fragment in the GLMs and in free imidazolylcobamides are compared in Fig. 12. The axial Co–N distances are 2.28 Å in the cyano cofactor and 2.34 Å in the methyl cofactor bound in the base-off/his-on mode [39,40], and should be compared to the corresponding distances in the Me- (2.09 Å [41]) and the CN- (1.968(9) Å [42]) imidazolylcobamides. Since the protein crystals contain the cofactor to 50% in hexacoordinated and to 50% in pentacoordinated form, the values of 2.28 Å and 2.34 Å in the CN and methyl cofactors were interpreted as the average of the very long distance (assumed to be 2.5 Å) of the pentacoordinated Co(II) species and the shorter distance of the hexacoordinated Co(III) species. Hence, they concluded

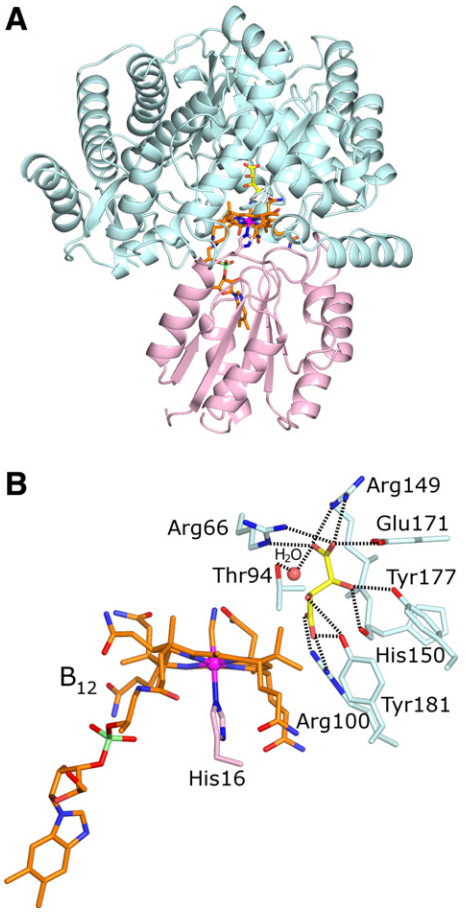

Fig. 11. The glutamate mutase structure, here the one reconstituted with CNCbl (PDB code 1CCW). (A) The ε domain is represented as cyan ribbons, the σ domain as pink ribbons, the tartrate as yellow sticks and the B_{12} as orange sticks. (B) An enlarged view to the two ligands emphasising the many H-bond interactions of the tartrate (in yellow) with residues of the ε domain.

that "the protein-bound B_{12} cofactor in the Co(III) state has an axial Co–N bond not much longer (if at all) than that deduced from crystallography of cobalamins" [38]. Comparison of the values of corresponding Co–N axial distances in imidazolylcobamides and cobalamins shows that they increase by about 0.07 Å in the latter (Fig. 12). Furthermore, the axial Co–N distance in the pentacoordinate Co(II)alamin of 2.13 Å [43] is very far from the value of 2.5 Å. It is shorter than that in MeCbl and it is longer than those in the Me and CN imidazolylcobamides as shown in Fig. 12, which also shows the dramatic distortion of the N coordination angles in the enzymes with respect to the N coordination in the isolated imidazolylcobamides. These two observations suggest that a lengthening of the Co–N bond should occur in the enzyme and that the value of 2.5 Å is unrealistically high (see Section 3.2) for the pentacoordinate Co(II) species in the enzymes. The lengthening in the enzyme may be evaluated on the basis of the EXAFS studies of the MeCbl–GLM, which yielded a longer Co–N distance of 2.18 Å [44], compared to that of 2.09 Å in the free methylimidazolylcobamide [41].

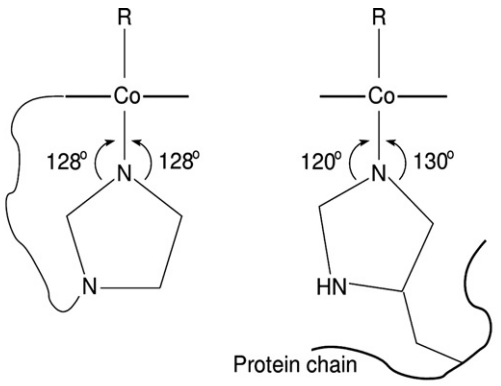

Co-N axial distances (Å)

R	Cba-Im	Cbl[a]	Cbl(base-off/his-on)[b]
CN	1.97[c]	2.04	2.28 2.18 (base-on)[d]
Me	2.09[e]	2.16	2.34
Ade	-	2.21[f]	2.22 (base-on)
Ado	-	2.24	2.22
Co(II)Cbl	-	2.13[g]	2.5 2.2-2.6 (base-on)[h]

[a] ref. 19, if not otherwise stated; [b] ref. 7, if not otherwise stated; [c] ref. 41; [d] ref. 55; [e] ref. 42; [f] ade = adeninylpentyl ; [g] ref. 43; [h] refs. 56-58, 60-61.

Fig. 12. Structures of the R–Co–N axial fragment in imidazolylcobamide (Cba-Im) and in the enzyme. The Co–N axial distances for some types of upper axial ligands of Cbl and Cba-Im are compiled.

Kratky and co-workers [45] reported the crystal structure of GLM at 1.9 Å resolution, reconstituted with AdoCbl and glutamate. The axial Co–N distance is 2.22 Å. The electron density was interpreted as the superposition of two conformations of the ribose moiety of 5′-deoxyadenosyl, one with the ribose in a C_2-*endo* conformation A (40%) and the other in a C_3-*endo* conformation B (60%). These are shifted so that the C5′ carbons are 1.7 Å apart and at a distance of 3.2 Å above the Co and 4.5 Å from Co, respectively. In the latter case, the C5′ carbon atom is displaced towards the substrate. The interpretation of this finding was that the C_2-*endo* conformation corresponds to the activated coenzyme, with a highly strained Co–C bond, and the C_3-*endo* conformation represents that of 5′-deoxyadenosine after the transfer of the H atom from the substrate.

The structural finding on AdoCbl-GLM was exploited in a study of the Co–C bond cleavage in GLM that combined the methods of quantum mechanics and molecular mechanics [46]. The quantum mechanics calculation was based on a restricted AdoCo(corrin)Im^+ model (Fig. 8A) while molecular dynamics used the full AdoCbl, including amino acid residues within 10 Å of any atom of the quantum system. This study showed that the protein in the closed substrate-bound form [34] strongly destabilizes the Co–C bond, whose bond dissociation energy (BDE) is reduced by 135 kJ/mol with respect to the vacuum. Theoretical analysis indicated that this catalytic effect can be divided in four components. The main contributions derive from the distortions induced by the protein in AdoCo(corrin)Im^+ (61 kJ/mol), particularly in the ribosyl moiety (in the Co–CH_2–C angle opening up to 138°) and from the differential stabilization of the Co(II) state (42 kJ/mol). The decrease in the BDE of 20 kJ/mol derives from the stabilization of the Ado radical bound at 3.2–3.4 Å from Co (cage effect) and 11 kJ/mol from stabilization of the surrounding protein in the Co(II) state. Thus, this study suggests that the Co–C cleavage is enhanced by the enzyme binding to Cob(II)alamin more favourably than to AdoCbl. Since no variation on the corrin ring geometry is observed on the basis of these calculations, the previously suggested mechanochemical trigger mechanism [47] is ruled out as well as the electronic influence of the axial Co–N lengthening induced by the protein [32,48] since this effect destabilizes the complex by less than 4 kJ/mol. These calculations point towards the previous suggestion [34,43,49,50] that catalysis comes from the stabilization of the homolysis products as a result of protein binding.

The structure of the Class III enzyme lysine 5,6-aminomutase (5,6-LAM) from *C. sticklandii* shows a dimer of αβ units, each of 80.8 kDa [51]. The larger α unit contains a TIM barrel as do MMCM, DD and GM. The β unit contains two domains one of which is a Rossmann-like domain. The structure was determined to 2.8 Å in the absence of the substrate. It shows the αβ unit in a conformation in which AdoCbl is located at the edge of the interface between the two units (Fig. 13). The distance between AdoCbl and the other cofactor, pyridoxal-5′-phosphate located in the putative active site, is ≈25 Å and thus, this substrate-free conformation corresponds to a precatalytic state suggesting large unit rearrangements upon substrate-binding to bring AdoCbl in contact with the active site. AdoCbl is present in base-off/His-on form with the nucleotide arm reaching into the Rossmann domain as in MetH, and Class I AdoCbl-dependent enzymes. The corrin side chains d and e interact with the Rossmann domain by several H-bonds while the Ado moiety forms H-bonds to the α unit. Thus, AdoCbl stabilizes the contact of the two protein units. The relative orientation of the TIM barrel and the Rossmann domain is different from the enzymes discussed above, a fact that is assumed to be linked to the precatalytic character of the observed conformation in which AdoCbl has to be kept outside the substrate-free active site to prevent undesired radical generation.

3.2. Class II enzymes

Both diol dehydratase (DD) and glycerol dehydratase (GD) catalyze the conversion of 1,2-propanediol, 1,2-ethanediol, and glycerol to propionaldehyde, acetaldehyde, and β-hydroxypropionaldehyde and water, respectively. Ethanolamine ammonia-lyase (EAL) catalyzes the conversion of ethanolamine to acetaldehyde and ammonia (Table 3). DD and GD are considered isoenzymes, even if their

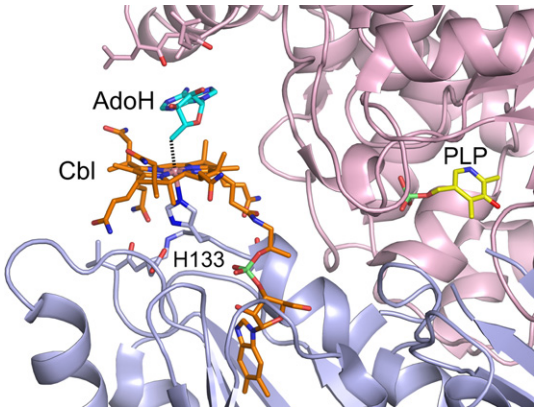

Fig. 13. Structure of lysine 5,6-aminomutase (5,6-LAM). The long distance of 2.6 Å between Co and the C5′ carbon atom of Ado's ribose group (dashed line) points to (partial) X-ray-induced reduction of this labile bond during data collection for which reason AdoCbl was modelled as Cbl and AdoH [51]. His 133 displaced dimethylbenzimidazole on the lower axial side of Co. The distance of Cbl to the other cofactor pyridoxal-5′-phosphate (PLP, in yellow) in the active site is ≈25 Å in this substrate-free structure (PDB code 1XRS).

specificity (as the enzyme names insinuate) is higher for 1,2-propanediol or glycerol, respectively. The X-ray structures of DD and GD have been reported, but that of EAL is not yet available even if there are several spectroscopic evidences that cobalamin is bound in the base-on form [7].

The X-ray structure of DD from *Klebsiella oxytoca* (220 kDa), reconstituted with CNCbl and 1,2-propanediol, was determined at 277 K to 2.2 Å resolution and represented the first reported X-ray structure of an AdoCbl-dependent enzyme, in which the coenzyme is bound to the protein in the base-on form, i.e. the 5,6-dimethylbenzimidazole of the nucleotide loop is coordinated to cobalt in the lower axial position [52]. The enzyme is a dimer of heterotrimers, $(\alpha\beta\gamma)_2$. In each trimer (Fig. 14A), the cobalamin is bound between the α and β subunits and five of its amide side chains form H-bonds with amino acids of the two subunits. The α subunit contains the $(\beta\alpha)_8$ barrel, where the 1,2-propanediol substrate and the essential cofactor, a K^+ ion, are deeply buried (Fig. 14B). The two hydroxyl groups of the substrate coordinate the potassium ion, which completes the hepta-coordination sphere with O atoms from some amino acid residues. The TIM barrel has an architecture similar to that where the substrate is located in Class II AdoCbl enzymes and in MetH. Although the cobalamin is bound in a quite different manner (see below) from the base-off/his-on mode found in MetH, the $(\beta\alpha)_8$ barrel may be considered a common feature for B_{12} enzymes, if the ribonucleotide reductase is excluded. The central part of the β subunit consists of a Rossmann fold, similar to that found for the Cbl-binding site in the other B_{12} based enzymes so far crystallographically characterized. This domain is in contact through several H-bonds with the lower part of the cobalamin in base-on form, with a Co–N axial bond length of 2.5 Å. No electron density

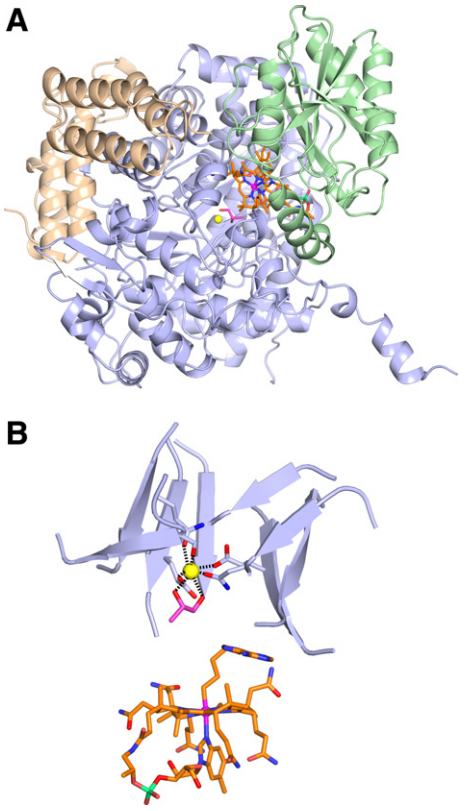

Fig. 14. Structure of diol dehydratase (DD). Panel (A) refers to the structure from data collected at 100 K (PDB code 1EGM) and shows one subunit of the dimeric enzyme. Each subunit consists of a trimer. The larger α-domain, a TIM barrel of 61 kDa, is shown in blue, the smaller β-domain (22 kDa), with α/β Rossmann fold, is shown in green and the smallest domain γ (16 kDa) in orange. (B) The propanediol and five amino acid residues from the inner part of the TIM barrel coordinate a potassium ion (shown in yellow). This structure refers to that of DD reconstituted with adeninylpentylCbl shown here in orange.

was detected on the CN axial group, suggesting that the cobalt atom is present as Co(II). However, when X-ray data were collected at 100 K (at 1.9 Å resolution) [53] the CN group was partially observable and the *trans* Co–N axial distance was found to be 2.18 Å, longer than that of 2.04 Å found in the free CNCbl [19]. This paper reported also the X-ray structure of DD reconstituted with the substrate and adeninylpentylcobalamin (AdeCbl), an inhibitor of DD, with data to 1.7 Å resolution collected at 100 K in the dark. The $(\alpha\beta\gamma)_2$ structure is similar to that found for CNCbl. AdeCbl was clearly identified and located between the α and β subunits, with its adenine ring parallel to the corrin over the C pyrrole ring (Fig. 14B). All the adenine N atoms, except the one bound to the pentyl group, form several H-bonds with amino acids of the α subunit. This strong binding of the upper axial ligand, in addition to the H-bonds formed by the amide side chains with the protein amino acids explains why AdeCbl is bound more tightly than AdoCbl by DD [54]. The axial fragment has Co–C and Co–N distances of 2.07 and 2.22 Å, respectively. These should be compared to the corresponding values of

1.96 and 2.21 Å found in the free AdeCbl [19]. When the data collection was performed at 100 K (1.8 Å resolution), after repeated illumination of the crystal with visible light, the electron density map clearly showed the adenine moiety still held close to the protein by H-bonds, whereas the electron density of the pentyl moiety disappeared [55]. This result suggested that the visible light cleaved the Co–C bond, with formation of the Cob(II)alamin with an axial Co–N distance of 2.16 Å and the adenine well fixed to the protein scaffold by H-bonds. Finally, the X-ray structure of the substrate-free form of DD reconstituted with CNCbl and K^+ at 100 K (1.9 Å resolution) [56] did not show that dramatic conformational changes in the protein occur upon binding of the substrate, if a tilt of about 3° of the β subunit is excluded. The K^+ ion is still heptacoordinate, two water molecules substituting the substrate hydroxyls in its coordination sphere. The Co–N axial distance is 2.25 Å, close to that of 2.18 Å found in the substrate-bound form. More generally, the binding of the substrate induces rather small distortion in the cobalamin. A modelling study led to the suggestion [56] that the Co–C bond becomes largely activated (labilized) by the binding of cobalamin to the apoenzyme, even in the absence of the substrate. This is in contrast to what occurs in B_{12} isomerases (Section 3.1) where the entrance of substrate significantly contributes to the activation of the Co–C bond homolysis [32,34,36,37]. The essential role of K^+ in the catalysis performed by DD was addressed in a DFT study [57] that supported the direct participation of K^+ in the 1,2 rearrangement of the substrate.

The X-ray structure at 100 K and 2.0 Å resolution of the recombinant GD from *Klebsiella pneumoniae*, isoenzyme of DD, in complex with CNCbl, 1,2-propanediol, and the essential K^+ ion, was reported [58]. It shows no large structural difference from that of DD. The electron density of the CN group was not detected and this, together with the very long Co–N axial bond of 2.5 Å, was interpreted as reduction of CNCbl to Cob(II)alamin. The corresponding substrate-free GD structure in complex with CNCbl and K^+ was also reported [59] (at 100 K, 2.5 Å resolution) and showed that the potassium ion is now hexacoordinate with a water molecule coordinating in place of the two OH groups of the diol. Again, the CN group was not detected and the axial Co–N distances in the two homotrimers are 2.5 and 2.6 Å, respectively.

3.3. B_{12} ribonucleotide reductase

Ribonucleoside triphosphate reductase (RTPR) catalyzes the reduction of ribonucleoside triphosphates to 2′-deoxyribonucleoside triphosphates. It is the only AdoCbl-dependent enzyme that does not catalyze a rearrangement. As in all ribonucleotide reductases (RNR), which are subdivided in three classes upon the kind of metallofactor, the latter serves to generate an active thiyl radical. In the case of RTPR, the activation process involves Co–C bond homolysis followed by transfer of a hydrogen atom from a Cys residue to the Ado radical to form 5′-deoxyadenosine and the thiyl radical. The other two classes use a diirontyrosyl and glycyl radical (generated by an FeS cluster and AdoMet), respectively, to produce the thiyl radical S· [60]. The thiyl radical initiates interaction with the substrate by abstracting a hydrogen atom from the 3′ carbon

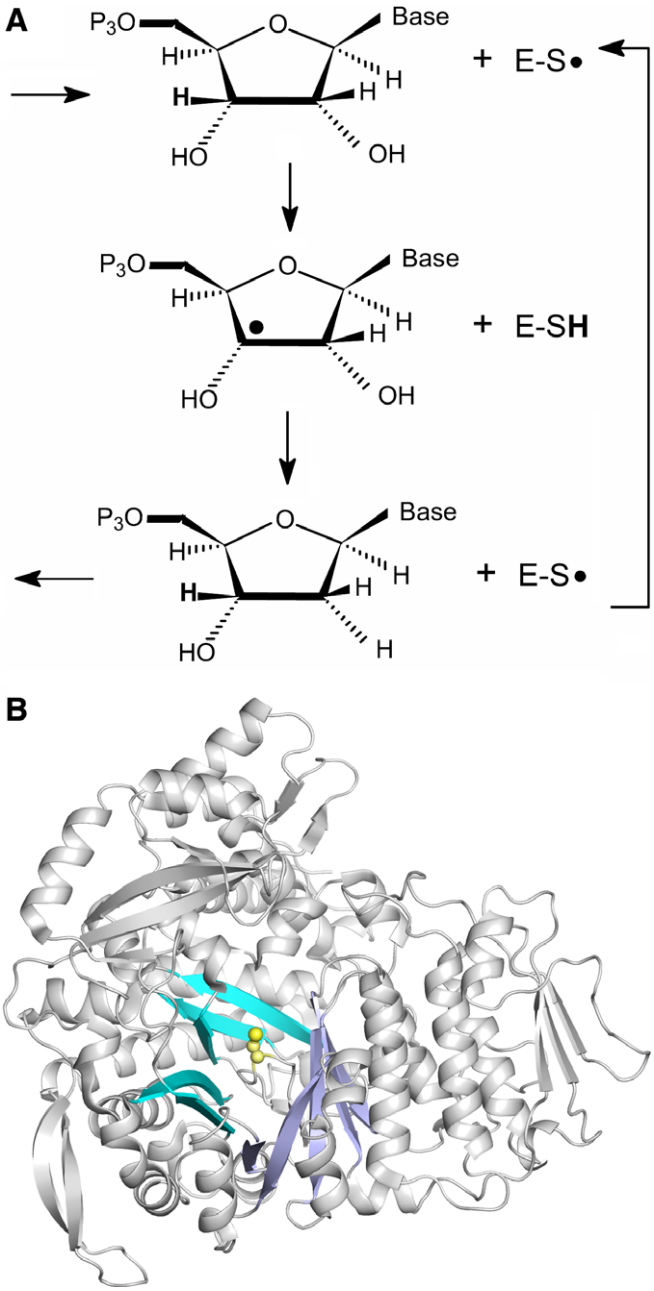

Fig. 15. The ribonucleoside triphosphate reductase structure and function. (A) A simplified scheme of the reaction in which the thiyl radical abstracts a hydrogen atom from the 3′ carbon of the substrate ribose moiety. (B) The structure of RTPR from *Lactobacillus leichmannii* (PDB code 1L1L). The cartoon representation highlights the protein core consisting of two β-sheets. Both sheets (one in cyan, one in blue) are built of five parallel strands and run antiparallel to each other. The essential Cys residue in the centre of the barrel is shown in yellow ball-and-stick representation.

of the substrate ribose moiety [61], according to the simplified scheme shown in Fig. 15A.

The X-ray crystal structure of RTPR from *Lactobacillus leichmannii* (80 kDa) both as the apoenzyme and in complex with AdeninylpentylCbl (AdeCbl), has been determined to 1.8 and 2.0 Å resolution, respectively [62]. The structure shows a core of a $(\alpha/\beta)_{10}$ barrel with two parallel five-stranded β sheets oriented antiparallel to each other. It differs significantly from the TIM barrel found in the B_{12} enzymes, in which the eight β-strands are parallel (Fig. 15B). However, it is more similar to that found in the di-ferric RNR [63]. The centre of the barrel contains the catalytic site, a finger-loop with the essential Cys residue which provides the thiyl radical. The coenzyme-binding domain, where Cbl is bound in the base-on form, shows no structural similarity to other B_{12}-binding domains, not even to that of Class II AdoCbl enzymes, which also bind the B_{12} coenzyme in the base-on form. The pentamethylene portion of AdeCbl is clearly attached to Co, whereas the electron density in the adenine region is ambiguous. Comparison of the structure of the AdeCbl-complexed protein with the apoenzyme indicates a slightly more closed conformation in the former.

4. Adenosyltransferase

We briefly mention an example of enzymes where cobalamin does not play the role of a cofactor but that of a substrate. Mammals have to convert dietary cobalamins to AdoCbl in the mitochondrion to obtain the coenzyme for MMCM. In the *de novo* biosynthesis pathway of AdoCbl in anaerobic bacteria, the Co–C bond formation is catalyzed by the ATP:co(I)rrinoid adenosyltransferase (CobA) which transfers the adenosyl group from MgATP to a variety of co(I)rrinoid substrates. The structure of this enzyme from *Salmonella typhimurium* in complex with MgATP and hydroxocobalamin (OH-Cbl) was determined at 2.1 Å resolution [64]. In the structure of the ternary complex, cobalamin interacts with the protein mainly by hydrophobic contacts and only few H-bonds of its polar side chains, consistent with the low substrate specificity of the enzyme. Cobalamin is bound with dimethylbenzimidazole as lower axial ligand but without an upper axial ligand, i.e. the initial hydroxyl group is lost and a pentacoordinate Co(II) is likely present (Fig. 16).

In the proposed mechanism, the initial Co(III) is reduced to Co(I) by two separate one-electron transfer steps, the first of which being performed externally to CobA. Co(I) is then able to conduct a nucleophilic attack on the adenosyl group of ATP to produce the final adenosylated Co(III). The way in which the protein activates the Co(II) for reduction to Co(I) has been the subject of intense studies since the redox potential for this transition is very low in free cobalamin. The current explanation implies a small rise of this potential upon binding of cob(II)alamin to the MgATP-CobA complex, involving the formation of a four-coordinate Co(II) intermediate

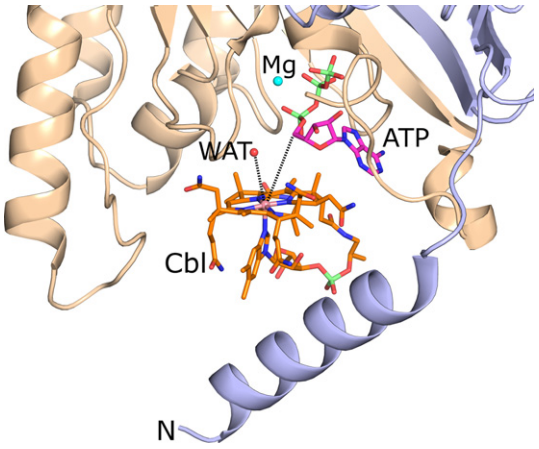

Fig. 16. Structure of CobA from *Salmonella typhimurium* (PDB code 1G64). Cobalamin bound to one subunit (in yellow) of the homodimeric enzyme is covered on its lower axial side by the flexible N-terminal helix of the other subunit (in blue) and shows few H-bond interactions with the protein. No upper axial ligand of Co is observed in the electron density map; a water molecule is present at a distance of 4.3 Å and the C5′ atom of the ribosyl moiety of ATP at 6.1 Å.

[65]. Subsequent binding of the electron transporter flavodoxin A will then result in the reduction of bound cob(II)alamin [66].

5. Vitamin B_{12} transport proteins

The transport of cobalamin from food to cells (Fig. 2) is accomplished by three successive proteins in mammals, haptocorrin (HC), gastric intrinsic factor (IF) and transcobalamin (TC) [11–13]. Upon initial uptake of Cbl from food, Cbl becomes bound in the stomach to salivary HC. After proteolysis of HC in the duodenum, Cbl is passed on to IF. Mucosal cells in the ileum absorb the IF–Cbl complex via endocytosis mediated by a specific receptor. In the enterocyte, the IF–Cbl complex is degraded and Cbl is transferred to TC which delivers Cbl to cells via the blood. Only the fraction of Cbl bound to TC (about 30%) is taken up via endocytosis by a specific receptor on most cell types. These cells, with the exception of hepatocytes, do not possess a receptor for HC that is also present in the blood. Hence, HC cannot facilitate cellular uptake of Cbl and may rather function as scavenger of harmful Cbl analogues in the body [12]. TC–Cbl is degraded in lysosomes to release Cbl for further conversion into its relevant coenzyme forms [15]. All three proteins carry a single Cbl molecule and show high affinity to the ligand [67], as shown by the K_d values for each protein given in Fig. 2. However, they differ in specificity for Cbl-analogues which are also produced by microorganisms [68]: specificity increases in the order HC $\ll$ TC $<$ IF [12]. The structures of human and bovine TC in complex with Cbl have recently been solved by X-ray crystallography [8]. They represent the prototype for the family of mammalian Cbl-transporters since structures have not been reported yet for IF or HC.

TC shows a two-domain architecture in which a larger N-terminal domain ("α-domain"), composed of 12 α-helices in an α_6–α_6 barrel and a short 3/10 helix, is connected by a flexible linker region to a smaller C-terminal domain ("β-domain") consisting mainly of two β-sheets (Fig. 17A). Cbl is bound in its base-on form and is almost completely buried between the two domains with the plane of the corrin ring approximately perpendicular to the domain interface. The mode of Cbl-binding to the transporter TC is distinct from that of binding to the aforementioned enzymes. A coordination bond between Co and the imidazole side chain of a histidine residue from the α-domain is observed (Fig. 17B), apart from numerous H-bond interactions between TC and the polar groups of Cbl and fewer hydrophobic interactions [8]. The histidine displaced the H_2O at the β side of H_2O–Cbl which was used in the preparation of the TC–Cbl complex. Contrary to the base-off/His-on mode described above for two classes of AdoCbl-dependent enzymes, TC exhibits the His-on feature on the axial side opposite the dimethylbenzimidazole base, thus leaving the α side of Cbl in the base-on form.

In bovine TC, continuous electron density is observed between His 175 Nε and the Co ion. The bond length averaged 2.13 Å over the five crystallographically independent molecules of two crystal forms of bovine TC. In the structure of human TC, His 173 is in a position to form the analogous coordination bond. However, the clear discontinuity in the electron density map (at 3.2 Å resolution) and the greater distance (2.8 Å) between the Nε nitrogen atom of His 173 and the Co ion, suggest the presence of a mix of forms with and without His-Co coordination. Reduction of hexacoordinate Co(III) to pentacoordinate Co(II) may have been induced by X-rays during data collection, as observed in a similar case of AdoCbl-dependent glutamate mutase [69], and may have led to the loss of His coordination in the case of TC. It is hypothesized that only human TC was affected because the loop preceding His 173 in human TC is three residues shorter than that in bovine TC and may generate a stress that facilitates detachment of the imidazole side chain.

The physiological function of the displacement of the axial ligand on the β-side of cobalamin by a protein residue is unknown. No experimental evidence exists so far for a role regarding the protection of Cbl against a damaging effect exerted by solvent molecules. It should be noted that the affinity of Co(III) to ligands increases in the order $H_2O \ll \text{imidazole} < N_3^- < CN^-$ [1] and thus, only a weak ligand like H_2O is displaced by the histidine residue but not stronger ligands, such as CN^-. Even after substitution of the original axial ligand, high flexibility of the histidine-hosting loop remains. Consequently, no substantial structural difference is expected between the His-off form, e.g. TC–(CN–Cbl), and the His-on form TC–(His–Cbl).

In view of the application of Cbl-based bioconjugates as imaging or therapeutic drugs, it is helpful to inspect the environment of Cbl in complex with human TC. The structure indicates that only the 5′-hydroxyl group on the ribose of Cbl's nucleotide moiety offers space for the attachment of larger molecules without disturbing the interactions between TC and Cbl (Fig. 17C). The attachment at the corrin side chains or the phosphate group will inevitably lead to impaired interactions [70]. The upper axial ligand position of the Co ion can accommodate ligands as well despite the resulting loss of the His coordination [70].

Modelling the primary sequence of IF and HC on the three-dimensional structure of TC suggested that their amino acid sequences are consistent with a Cbl-binding mode similar to that observed for TC [71]. A comparison of the crystallographic model of TC with the two theoretical models of IF and HC points to some key residues responsible for the observed differences in affinity of the three transporters to Cbl analogues that show modifications on the nucleotide moiety of genuine Cbl. The elevated specificity of IF and TC for Cbl is thought to provide

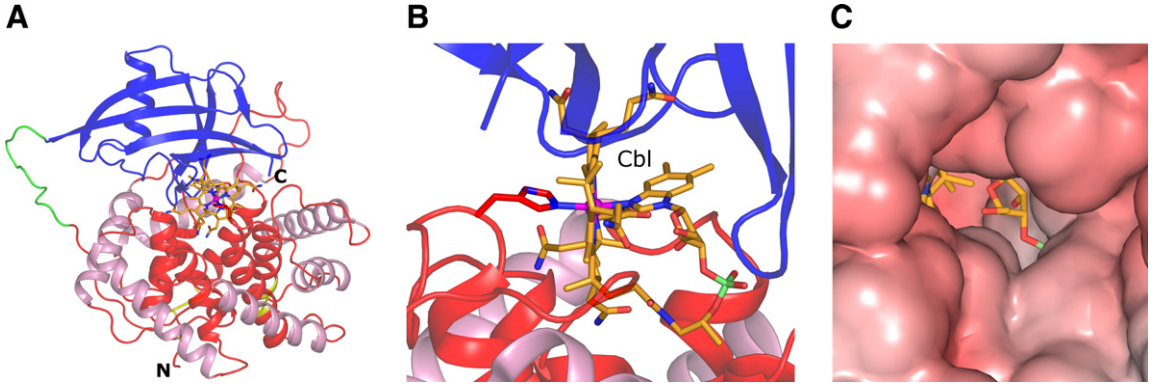

Fig. 17. The structure of transcobalamin, the protein that transports cobalamin through the blood. (A) The two-domain structure of TC. (B) Cobalamin in base-on form bound to bovine TC (PDB code 2BB6) is shown in orange sticks and reveals the unusual Co-coordination of a histidine residue from the upper axial side of the corrin ring. (C) The surface of human TC (PDB code 2BB5) which is accessible to a spherical solvent molecule of 1.4 Å radius. The surface possesses a slightly negative electrostatic potential and allows easy access to cobalamin at its ribose moiety.

protection against those analogues which might harmfully block the active site of the above mentioned enzymes if they were transported to cells with the same efficiency as genuine Cbl.

The B_{12} transport in mammals occurs as sketched in Fig. 2, whereas in *E. coli* (and other Gram-negative bacteria) the B_{12} transmembrane import is carried out by the B-twelve-uptake (Btu) system consisting of an outer membrane transporter BtuB and an ATP-binding cassette (ABC) transporter BtuCDF located in the inner membrane. The crystal structure of BtuB was reported to 3.1 Å resolution [72] and recently solved to 2.1 Å resolution in complex with the C-terminal domain of the inner membrane protein TonB [73]. The protein consists of a 22-stranded β-barrel spanning the outer membrane and enclosing a globular luminal domain (Fig. 18A). A mechanical pulling model is suggested for cobalamin transport through the barrel uppon binding of the TonB domain to the N-terminal β-strand ("Ton-box") of BtuB. The ABC transporters are membrane proteins which couple ATP hydrolysis to translocation of divers substrates across the cell membrane. In most bacteria, a periplasmic substrate-binding protein is employed to deliver the substrate to the transmembrane domains. In the $BtuC_2D_2F$ transporter, two BtuC domains are membrane-spanning subunits, each with one BtuD domain attached on the cytoplasmic side [74], while BtuF is the cognate periplasmic protein. The crystal structure of BtuF of *E. coli* has been reported in complex with CNCbl at 2.0 Å resolution [75,76]. The structure of BtuF consists of two similar α/β sandwich domains linked by an α-helix (Fig. 18B). CNCbl is bound in base-on form within a large cleft in the domain interface with its upper axial side facing the C-terminal domain. This domain, built of a parallel four-stranded β-sheet and five α-helices, is structurally homologous to the B_{12}-binding domain in all B_{12} enzymes but RTPR. In these enzymes, however, the homologous domain faces the lower axial side of Cbl.

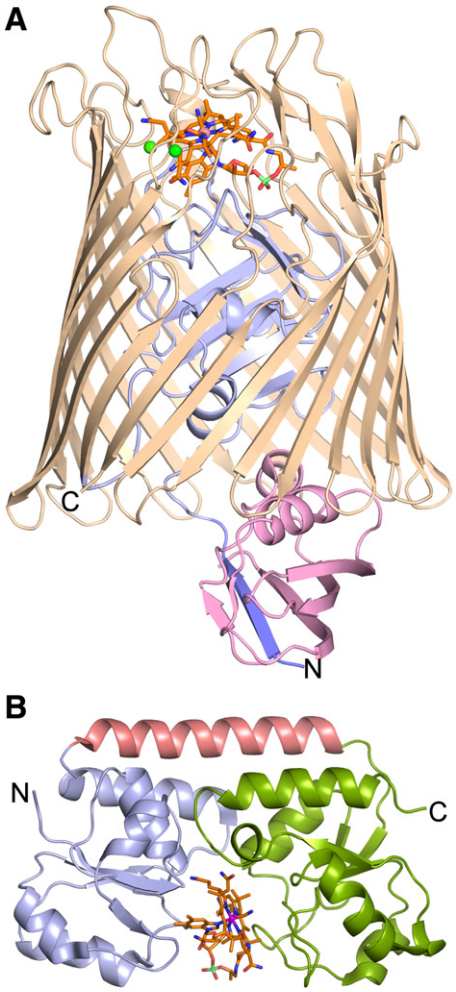

Fig. 18. Transmembrane import of cobalamin into *Escherichia coli*. (A) The outer membrane transporter BtuB (PDB code 2GSK). The transmembrane β barrel surrounds the luminal domain (in blue). Binding of CNCbl on the extracellular entrance (top) is facilitated by two calcium ions (green spheres). The C-terminal domain of TonB on the periplasmic side is shown in pink. (B) The structure of the periplasmic cobalamin-binding protein BtuF (PDB codes 1N4A, 1N2Z). CNCbl is bound between the N-terminal domain (in blue) and the C-terminal domain (in green) connected by a long α-helix (in red).

6. Conclusions

This short review has outlined the enormous impact of crystallography on the development of B_{12} biochemistry and enzymology. The usefulness of crystallography is also evident in the design of B_{12}-based conjugates as imaging agents or cytotoxic drugs in medical applications [77] as the molecular basis for the transport of B_{12} in the body are coming to light.

A lot of experimental and theoretical work has already been done to assess the influence of cobalamin's axial ligands and the protein environment on the organometallic chemistry of cobalt and its stability in a given oxidation state, as reviewed here. Based on the structures available to date, it appears that regarding transport proteins, Cbl prefers to bind in its base-on form. Instead, the dominating form when bound to enzymes is the base-off form. The reason behind this difference and in particular the function of the histidine substitution for dimethylbenzimidazole in some structures with Cbl in base-off form is still a matter of investigation.

Furthermore, the way by which AdoCbl enzymes catalyze the Co–C bond homolysis 10^{12} times faster than the free coenzymes is still unclear. Analogously, the intracellular processes leading from endocytosed TC–Cbl to the formation of AdoCbl in mitochondria as well as of MeCbl in the cytosol are not yet fully understood. More contributions from crystallography are certainly expected in elucidating the role of B_{12} in the mechanism of carbon dioxide fixation in anaerobic acetogenic bacteria and methanogenic archaea as well as in the reductive dehalogenation of chlorinated hydrocarbons.

References

[1] J.M. Pratt, The Inorganic Chemistry of Vitamin B12, Academic Press, London, 1972.
[2] E.L. Rickes, N.G. Brink, F.R. Koniuszy, T.R. Wood, K. Folkers, Science 107 (1948) 396.
[3] E.L. Smith, Nature 162 (1948) 144.
[4] D.C. Hodgkin, J. Kamper, M. MacKay, J. Pickworth, Nature 266 (1956) 1663.
[5] D.C. Hodgkin, J. Kamper, J. Lindsay, M. MacKay, J. Pickworth, J.H. Robertson, C.B. Shoemaker, J.G. White, R.J. Prosen, K.N. Trueblood, Proc. R. Soc. Lond. A242 (1957) 228.
[6] R. Banerjee, S.W. Ragsdale, Annu. Rev. Biochem. 72 (2003) 209.
[7] K.L. Brown, Chem. Rev. 105 (2005) 2075.
[8] J. Wuerges, G. Garau, S. Geremia, S.N. Fedosov, T.E. Petersen, L. Randaccio, Proc. Natl. Acad. Sci. USA 103 (2006) 4386.
[9] J.M. McGreevy, M.J. Cannon, C.B. Grissom, J. Surg. Res. 111 (2003) 38.
[10] G. Russell-Jones, K. McTavish, J. McEwan, J. Rice, D. Nowotnik, J. Inorg. Biochem. 98 (2004) 1625.
[11] B. Kräutler, D. Arigoni, B.T. Golding (Eds.), Vitamin B_{12} and B_{12} Proteins, Wiley–VCH, Weinheim, 1998.
[12] R. Banerjee, Chemistry and Biochemistry of B12, John Wiley & Sons, New York, 1999.
[13] B. Seetharam, S. Bose, N. Li, J. Nutr. 129 (1999) 1761.
[14] E.V. Quadros, Y. Nakayama, J.M. Sequeira, Biochem. Biophys. Res. Commun. 327 (2005) 1006.
[15] R. Banerjee, ACS Chem. Biol. 1 (2006) 149.
[16] R.G. Matthews, Acc. Chem. Res. 34 (2001) 681.
[17] S.W. Ragsdale, in: R. Banerjee (Ed.), Chemistry and Biochemistry of B12, John Wiley & Sons, New York, 1999, pp. 633–653.
[18] K. Sauer, R.K. Thauer, in: R. Banerjee (Ed.), Chemistry and Biochemistry of B12, John Wiley & Sons, New York, 1999, pp. 655–680.
[19] L. Randaccio, S. Geremia, G. Nardin, J. Wuerges, Coord. Chem. Rev. 250 (2006) 1332.
[20] J.C. Evans, D.P. Huddler, M.T. Hilgers, G. Romanchuk, R.G. Matthews, M.L. Ludwig, Proc. Natl. Acad. Sci. USA 101 (2004) 3729.
[21] J.T. Jarrett, C.Y. Choi, R.G. Matthews, Biochemistry 36 (1997) 15739.
[22] C.L. Drennan, S. Huang, J.T. Drummond, R.G. Matthews, M.L. Ludwig, Science 266 (1994) 1669.
[23] M. Dixon, S. Huang, R.G. Matthews, M.L. Ludwig, Structure 4 (1996) 1263.
[24] V. Bandarian, K.A. Pattridge, B.W. Lennon, D.P. Huddler, R.G. Matthews, M.L. Ludwig, Nat. Struct. Biol. 9 (2002) 53.
[25] V. Bandarian, M.L. Ludwig, R.G. Matthews, Proc. Natl. Acad. Sci. USA 100 (2003) 8156.
[26] K.P. Jensen, U. Ryde, J. Am. Chem. Soc. 125 (2003) 13970.
[27] J.T. Jarrett, M. Amaratunga, C.L. Drennan, J.D. Scholten, R.H. Sands, M.L. Ludwig, R.G. Matthews, Biochemistry 35 (1996) 2464.
[28] C.H. Hagemeier, M. Krüer, Rudolf K. Thauer, E. Warkentin, U. Ermler, Proc. Natl. Acad. Sci. USA, 103 (2006) 18917.
[29] R. Banerjee, Chem. Rev. 103 (2003) 2083.
[30] T. Toraya, Chem. Rev. 103 (2003) 2095.
[31] T. Toraya, Cell. Mol. Life Sci. 57 (2000) 106.
[32] F. Mancia, N.H. Keep, A. Nakagawa, P.F. Leadlay, S. McSweeney, B. Rasmussen, P. Bösecke, O. Diat, P.R. Evans, Structure 4 (1996) 339.
[33] R. Jansen, F. Kalousek, W. A Fenton, L.E. Rosenberg, F.D. Ledley, Genomics 4 (1989) 198.
[34] F. Mancia, P.R. Evans, Structure 6 (1998) 711.
[35] F. Mancia, G.A. Smith, P.R. Evans, Biochemistry 38 (1999) 7999.
[36] J.M. Pratt, Chem. Soc. Rev. 14 (1985) 161.
[37] B.P. Hay, R.G. Finke, J. Am. Chem. Soc. 109 (1987) 8012.
[38] R. Reitzer, K. Gruber, G. Jogl, U.G. Wagner, H. Bothe, W. Buckel, C. Kratky, Structure 7 (1999) 891.
[39] M. Tollinger, C. Eichmüller, R. Konrat, M.S. Huhta, E.N.G. Marsh, B. Kräutler, J. Mol. Biol. 309 (2001) 777.
[40] B. Hoffmann, M. Tollinger, R. Konrat, M.S. Huhta, E.N.G. Marsh, B. Kräutler, ChemBioChem 2 (2001) 643.
[41] B. Kräutler, R. Konrat, E. Stupperich, G. Färber, K. Gruber, C. Kratky, Inorg. Chem. 33 (1994) 4128.
[42] M. Fasching, W. Schmidt, B. Kräutler, E. Stupperich, A. Schmidt, C. Kratky, Helv. Chim. Acta 83 (2000) 229.
[43] B. Kraeutler, W. Keller, C. Kratky, J. Am. Chem. Soc. 111 (1989) 8936.
[44] F. Champloy, G. Jogl, R. Reitzer, W. Buckel, H. Bothe, B. Beatrix, G. Broeker, A. Michalowicz, W. Meyer-Klaucke, C. Kratky, J. Am. Chem. Soc. 121 (1999) 11780.
[45] K. Gruber, R. Reitzer, C. Kratky, Angew. Chem., Int. Ed. 40 (2001) 3377.
[46] K.P. Jensen, U. Ryde, J. Am. Chem. Soc. 127 (2005) 9117.
[47] J. Halpern, Science 227 (1985) 869.
[48] D.J.A. De Ridder, E. Zangrando, H.B. Burgi, J. Mol. Struct. 374 (1996) 63.
[49] R. Banerjee, Chem. Biol. 4 (1997) 175.
[50] R.G. Finke, in: B. Kräutler, D. Arigoni, B.T. Golding (Eds.), Vitamin B_{12} and B_{12} Proteins, Wiley–VCH, Weinheim, 1998 (Chapter 25).
[51] F. Berkovitch, E. Behshad, K.-H. Tang, E.A. Enns, P.A. Frey, C.L. Drennan, Proc. Natl. Acad. Sci. USA 101 (2004) 15870.
[52] N. Shibata, J. Masuda, T. Tobimatsu, T. Toraya, K. Suto, Y. Morimoto, N. Yasuoka, Structure 7 (1999) 997.
[53] J. Masuda, N. Shibata, Y. Morimoto, T. Toraya, N. Yasuoka, Structure (London) 8 (2000) 775.
[54] T. Toraya, K. Ushio, S. Fukui, H.P.C. Hogenkamp, J. Biol. Chem. 252 (1977) 963.
[55] J. Masuda, N. Shibata, Y. Morimoto, T. Toraya, N. Yasuoka, J. Synchrotron Rad. 8 (2001) 1182.
[56] N. Shibata, J. Masuda, Y. Morimoto, N. Yasuoka, T. Toraya, Biochemistry 41 (2002) 12607.
[57] T. Toraya, K. Yoshiawa, M. Eda, T. Yamabe, J. Biochem. 126 (1999) 650.
[58] M.A. Yamanishi, M. Yunoki, T. Tobimatsu, H. Sato, J. Matsui, A. Dokiya, Y. Iuchi, K. Oe, K. Suto, N. Shibata, Y. Morimoto, N. Yasuoka, T. Toraya, Eur. J. Biochem. 269 (2002) 4484.
[59] D.-I. Liao, G. Dotson, I. Turner, L. Reiss, M. Emptage, J. Inorg. Biochem. 93 (2003) 84.
[60] A. Jordan, P. Richard, Annu. Rev. Biochem. 67 (1998) 71.
[61] J. Stubbe, W.A. van der Donk, Chem. Rev. 98 (1998) 705.
[62] M.D. Sintchak, G. Arjara, B.A. Kellogg, J. Stubbe, C.L. Drennan, Nat. Struct. Biol. 9 (2002) 293.
[63] M. Eriksson, U. Uhlin, S. Ramaswamy, M. Ekberg, K. Regnström, B.-M. Sjöberg, H. Eklund, Structure 5 (1997) 1077.
[64] C.B. Bauer, M.V. Fonseca, H.M. Holden, J.B. Thoden, T.B. Thompson, J.C. Escalante-Semerena, I. Rayment, Biochemistry 40 (2001) 361.
[65] T.A. Stich, M. Yamanishi, R. Banerjee, T.C. Brunold, J. Am. Chem. Soc. 127 (2005) 7660.
[66] N.R. Buan, J.C. Escalante-Semerena, J. Biol. Chem. 280 (2005) 40948.
[67] S.N. Fedosov, L. Berglund, N.U. Fedosova, E. Nexø, T.E. Petersen, J. Biol. Chem. 277 (2002) 9989.
[68] J.F. Kolhouse, R.H. Allen, J. Clin. Invest. 60 (1977) 1381.
[69] F. Champloy, K. Gruber, G. Jogl, C. Kratky, J. Synchrotron Rad. 7 (2000) 267.
[70] P.M. Pathare, D.S. Wilbur, S. Heusser, E.V. Quadros, P. McLoughlin, A.C. Morgan, Bioconjugate Chem. 7 (1996) 217.
[71] J. Wuerges, S. Geremia, L. Randaccio, submitted for publication.
[72] D.P. Chimento, A.K. Mohanty, R.J. Kadner, M.C. Wiener, Nat. Struct. Biol. 10 (2003) 394.
[73] D.D. Shultis, M.D. Purdy, C.N. Banchs, M.C. Wiener, Science 312 (2006) 1396.
[74] K.P. Locher, A.T. Lee, D.C. Rees, Science 296 (2002) 1091.
[75] N.K. Karpowich, H.H. Huang, P.C. Smith, J.F. Hunt, J. Biol. Chem. 278 (2003) 8429.

[76] E.L. Borths, K.P. Locher, A.T. Lee, D.C. Rees, Proc. Natl. Acad. Sci. USA 99 (2002) 16642.
[77] S. Kunze, F. Zobi, P. Kurz, B. Spingler, R. Alberto, Angew. Chem., Int. Ed. 43 (2004) 5025.
[78] S. Dong, R. Padmakumar, R. Banerjee, T.G. Spiro, J. Am. Chem. Soc. 121 (1999) 7063.
[79] D. Lexa, J.M. Saveant, J. Am. Chem. Soc. 100 (1978) 3220.
[80] B.M. Martin, R.G. Finke, J. Am. Chem. Soc. 114 (1992) 585.
[81] L. Randaccio, M. Furlan, S. Geremia, M. Slouf, I. Srnova, D. Toffoli, Inorg. Chem. 39 (2000) 3403.
[82] L. Ouyang, P. Rulis, W.Y. Ching, G. Nardin, L. Randaccio, Inorg. Chem. 43 (2004) 1235.